 doi:10.20944/preprints202204.0272.v1

Article

Silent Antibodies Start Talking: Enhanced Lateral Flow Serodiagnosis with Two-Stage Incorporation of Labels into Immune Complexes

Dmitriy V. Sotnikov[1,*], Nadezhda A. Byzova[1], Anatoly V. Zherdev[1], Youchun Xu[2] and Boris B. Dzantiev[1]

[1] A.N. Bach Institute of Biochemistry, Research Center of Biotechnology of the Russian Academy of Sciences, Leninsky prospect 33, Moscow 119071, Russia; nbyzova@mail.ru (N.A.B); zherdev@inbi.ras.ru (A.V.Z.); xyc2012@mail.tsinghua.edu.cn (YX); dzantiev@inbi.ras.ru (B.B.D.)

[2] State Key Laboratory of Membrane Biology, Department of Biomedical Engineering, School of Medicine, Tsinghua University, Beijing 100084, China.

* Correspondence: sotnikov-d-i@mail.ru; Tel.: +7-495-9543142

Abstract: Nowadays, the presence of pathogen-specific antibodies in the blood is widely controlled by a serodiagnostic technique based on the lateral flow immunoassay (LFIA). However, its common one-stage format with an antigen immobilized in the binding zone of a test strip and a nanodispersed label conjugated with immunoglobulin-binding proteins is associated with risks of very low analytical signals. It is caused by the presence of non-specific immunoglobulins in very large excess to the target antibodies in the tested samples thus decreasing their binding with the detected labels. In this study, the first stage of the immunochromatographic serodiagnosis was carried out in its traditional format using a conjugate of gold nanoparticles with staphylococcal immunoglobulin-binding protein A and an antigen immobilized on a working membrane. At the second stage, a labeled immunoglobulin-binding protein was added, which enhanced the coloration of the bound immune complexes. The use of two separated steps, binding of specific antibodies, and further coloration of the formed complexes allowed a significant reducing the influence of non-specific immunoglobulins on the assay results. The proposed approach was applied for the serodiagnosis using a recombinant RBD protein of SARS-CoV-2. As a result, an increase in the intensity of test zone coloration by more than two orders of magnitude was demonstrated, which enabled to significantly reduce false-negative results. When testing a panel of 16 positive and 8 negative serum samples, the diagnostic sensitivity of the LFIA was 62.5% for the common format and 100% for the enhanced format; the diagnostic specificity of both variants was 100%.

Keywords: immunochromatography; test strips; RBD protein; COVID-19; coronavirus

1. Introduction

Detection of pathogen-specific antibodies in the blood (serodiagnosis) plays a key role in the diagnostics of many infectious diseases. The advantages of this method are caused by the choice of a specific biomatrix to be tested (in contrast to the determination of viruses or bacteria in different organs and tissues) and the similarity of the assay protocols for different infections [1]. Microplate-based enzyme-linked immunosorbent assays (ELISAs), agglutination tests, and other immunoassay formats are successfully used for this purpose in medical diagnostics [2-4]. The current trend in the development of diagnostic tools is simplification and acceleration of the testing procedure. The lateral flow immunoassay (LFIA) is of the most relevant immunoassay formats given the availability of industrial facilities for the wide manufacturing of diagnostic kits. Multimebrane composites (test strips) with preliminary applied immune reactants and colored nanoparticles as detected labels provide maximum reducing manipulations of an operator. Contact of a test strip with the tested sample initiates the lateral flow of the immune reactants along the membranes and the assay results can be visualized in 10-15 min by the coloration of

 doi:10.20944/preprints202204.0272.v1

the test strip zones [5]. Successful development of the LFIA-based serodiagnosis of various deceases is presented in several publications [6-10]. As its additional application, the assessment of the vaccine effectiveness and the organism's protection against infections can be mentioned [11, 12].

The recent COVID-19 pandemic also caused the necessity of serodiagnostic LFIAs, which were successfully developed and commercialized by different groups and organizations [13, 14]. Nevertheless, the development and practical application of a serodiagnostic LFIA are accomplished by significant limitations. The percentage of the infection cases revealed by the LFIA serodiagnosis is often inferior to that detected by instrumental immunoassays such as the ELISA. The main factor causing this obstacle is the need to detect specific antibodies with low concentrations in the presence of great excess of total immunoglobulins [15].

Serodiagnosis is typically implemented using immunoglobulin-binding proteins such as anti-species antibodies or bacterial protecting compounds (staphylococcal protein A, streptococcal protein G, etc.). In the common LFIA format, they are immobilized on colored nanoparticles, applied on a test strip, and form complexes with all immunoglobulins including ones specific to the target pathogen during lateral flow. The resulting complexes interact with the antigen immobilized in the test zone (TZ) of the strip, whereas unbound compounds move across this zone. Therefore, the coloration of the TZ indicates the presence of specific antibodies in the tested sample [8, 16-18]. However, non-specific immunoglobulins block binding sites at the surface of nanoparticles and only a minor part of specific antibodies can form labeled complexes at the TZ. This differs from the ELISA-based serodiagnosis where non-bound antibodies can be removed (washed) before the inclusion of labels into immune complexes. Such limited binding leads to a significant percentage of false-negative results that are often indicated during the validation of these assays [19, 20].

The possibility to change the order of the immune complexes formation was considered in alternative serodiagnostic LFIAs [19, 21, 22]. As a result, some limitations were noted in these approaches. For example, the inverted LFIA format where the antigen is immobilized on label particles and the immunoglobulin-binding protein is adsorbed on the working membrane allows for the binding of more immunoglobulins than in the traditional LFIA format. Nevertheless, in this case, the interference of non-specific immunoglobulins is not eliminated [23-25]. One of the approaches to eliminate their influence is the “double antigen sandwich” LFIA format based on the antibody polyvalence [22, 26-28]. However, because of the side formation of polyvalent complexes, the efficiency of this format strongly depends on the ratio of the reagents [15]. The use of more sensitive labels or signal amplification by aggregation or catalysis was also considered [29-32]. The improvement achieved by these methods is associated with significant changes in test strips production. Therefore, they can be implemented in mass practice only after solving additional tasks such as stabilization of new reactants and prevention of their non-specific interactions.

Therefore, the improvement of the common serodiagnostic LFIA based on the conjugates of immunoglobulin-binding proteins with traditional nanodisperse labels ensuring an increase of labeled immune complexes in the TZ is in great demand. In the present study, a two-stage serodiagnostic LFIA is proposed. This method includes the common LFIA (the first stage) and additional labeling of bound specific immunoglobulins by a conjugate of gold nanoparticles with an immunoglobulin-binding protein (the second stage). This approach was performed for the serodiagnostic of COVID-19 infection and demonstrated the enhancement of the coloration intensity by two orders of magnitude compared to the common LFIA format, which significantly reduces the likelihood of false-negative results.

2. Materials and Methods

2.1. Chemicals, Materials, and Apparatuses

Preprints (www.preprints.org) | NOT PEER-REVIEWED | Posted: 28 April 2022 doi:10.20944/preprints202204.0272.v1

The recombinant receptor-binding domain (RBD) of SARS-CoV-2 spike protein [33] was kindly provided by Dr. I.I. Vorobiev. The monoclonal antibodies (MAb) to RBD, clone RBD5313, were from HyTest (Moscow, Russia). Goad anti-mouse immunoglobulins (GAMI) and a conjugate of recombinant staphylococcal protein A with gold nanoparticles (pA–GNP) were from Arista Biologicals (Allentown, USA). The polyclonal anti-human antibodies labeled with horseradish peroxidase were from Imtek (Moscow, Russia). NIBSC Anti-SARS-CoV-2 Antibody Diagnostic Calibrant reagent was purchased from National Institute for Biological Standards and Control (Hertfordshire, UK). Human serum was kindly provided by Dr. S.F. Biketov (State Research Center of Applied Microbiology and Biotechnology, Obolensk, Russia) and collected in the frame of earlier studies [31] from volunteers and patients after obtaining written and informed consent. The pooled negative serum was prepared by mixing 10 sera from donors without symptoms of respiratory diseases and antibodies against RBD of SARS-CoV-2 according to enzyme immunoassay.

Bovine serum albumin (BSA), sucrose, poly(vinyl formal), Tris, Tween 20, Triton X-100, 3,3,5,5′-tetramethylbenzidine (TMB), hydrogen peroxide (H_2O_2, 30%), were from Sigma Aldrich (St. Louis, USA). All salts and acids were from Khimmed (Moscow, Russia). All solutions were prepared using deionized water produced by Milli-Q (Billerica, USA).

Nitrocellulose working membranes (CNPC-15), glass fiber conjugate membranes (PT-R7), sample membranes (GFB-R4), and adsorbent membranes (AP045) were purchased from Advanced Microdevices (Ambala Cantt, India). The 96-well transparent polystyrene microplates for ELISA were purchased from Corning Costar (Tewksbury, MA, USA).

2.2. Characterization of pA–GNP

For transmission electron microscopy (TEM), pA–GNP solution was applied to 300-mesh grids (Pelco International; Redding, CA, USA) coated with a poly(vinyl formal) film. Then the film was placed on the glass and exposed to 0.15% v/v solution of formvar in chloroform. The images were obtained with a JEM CX-100 microscope (Jeol, Tokyo, Japan) at 80 kV and analyzed by the Image Tool software (University of Texas, Health Science Center, San Antonio, TX, USA).

The hydrodynamic size of pA–GNP was measured using a Zetasizer Nano (Malvern Pananlytical; Malvern, UK) at 25 °C for 10 s at a scattering angle of 173°.

2.3. Preparation of test strips

GAMI (0.5 mg/mL) and RBD (0.5-1.0 mg/mL) in 50 mM K-phosphate buffer with 100 mM NaCl, pH 7.4 (PBS), were applied to the control zone (CZ) and the TZ of the working membrane, respectively, by Image Technology IsoFlow dispenser (Lebanon, NH, USA) at a loading of 0.12 μL/mm. The pA-GNP conjugate (optical density at 520 nm (OD_{520}) = 2-20) containing 1.0% v/v Tween 20 was applied to the conjugate membrane (0.8 μL/mm). Both membranes were dried at room temperature for 12 h and composed together with sample and absorbent membranes to multimembrane sheets. Finally, test strips (of 3.5 mm width) were obtained by cutting sheets with an automatic Index Cutter-1 guillotine (A-Point Technologies; Gibbstown, NJ, USA) and stored at room temperature in zipper bags.

2.4. Lateral flow immunoassay

The common LFIA was performed at room temperature as follows:

- the test strip was placed on a horizontal surface,
- A volume of 60 μL sample was applied to the sample membrane,
- the strip was incubated for 5 min,
- A volume of 20 μL TTBSA buffer (10 mM Tris, 0.25% w/v BSA, 0.25% w/v sucrose, 1.0% v/v Tween 20, 0.05% w/v NaN_3, pH 8.5) was applied to the sample membrane;
- the strip was incubated for 5 min.

Preprints (www.preprints.org) | NOT PEER-REVIEWED | Posted: 28 April 2022 doi:10.20944/preprints202204.0272.v1

The enhanced LFIA was started as described above for the common LFIA. Then, 2 μL of the pA–GNP conjugate was applied to the bottom edge of the working membrane. After that, 60 μL of TTBSA was applied and the test strip was incubated for 5 min.

Finally, images of the test strips were obtained using a CanoScan 9000F scanner (Canon, Tochigi, Japan), and the intensities of TZ coloration were measured in grayscale mode using TotalLab TL120 software (Nonlinear Dynamics, Newcastle, UK). Each sample was tested in duplicate. The limit of detection (LOD) was determined as the concentration providing the coloration of the TZ higher than the sum of the average coloration intensity and three standard deviations for a blank probe.

2.5. ELISA of human serum

RBD (1 μg/mL, in PBS) was incubated in the microplate wells at 4 °C overnight. The wells were washed 4 times to remove unbound molecules using PBS with 0.05% v/v Triton X-100 (PBST). After that, serum diluted with PBST (1:25-1:50000) was added and the microplate was incubated for 1 h at 37 °C. Then, the microplate was washed again and anti-human antibodies labeled with horseradish peroxidase (dilution of 1:3000 in PBST) were added to each well. The microplate was incubated for 1 h at 37 °C. After washing the microplate as described above, the enzyme activity of the bound peroxidase label was determined. For this, the substrate mixture containing 0.4 mM TMB and 3 mM H_2O_2 in 40 mM sodium citrate buffer, pH 4.0, was added. After incubation at room temperature for 15 min, the reaction was stopped by adding 1 M H_2SO_4 to the substrate mixture (v/v = 1:2). Finally, A_{450} was measured using a Zenyth 3100 microplate photometer (Anthos Labtec Instruments, Wals, Austria).

3. Results and discussion

3.1. Consideration of the proposed assay format

The serodiagnostic LFIA can be implemented in several formats, which differ in the order of arranging the reagents on the membranes and the composition of the resulting complexes [19, 21, 22]. The most common format is based on the use of labeled immunoglobulin-binding proteins as reagents to visualize immune complexes. Pathogen antigens are immobilized in the TZ and interact with specific antibodies there, which leads to label binding.

The assay proposed in this study was firstly implemented in the same manner as the common LFIA (Fig. 1, stage 1). In the case of the presence of specific antibodies in a tested blood sample, colored complexes of the immobilized antigen, specific antibodies, and a labeled immunoglobulin-binding protein are formed in the TZ. Let's consider this process in more detail to clarify points for its improvement. The concentration of IgG as the main class of immunoglobulins in human blood is normally about 6-20 mg/mL [34] while the sorption capacity of gold nanoparticles with a diameter of 30 nm (as the optimal LFIA label) does not exceed 5 μg/mL per unit of the OD [35]. Therefore, even if the OD of the conjugate is 10, it binds less than 1% of the IgG fraction from the sample. The same proportion is actual for specific anti-pathogen antibodies. Theoretically, the problem can be solved by concentrating the conjugate. However, an increase in the concentration of gold nanoparticles promotes their aggregation, which leads to overlapping of binding centers and a stability decrease. Therefore, a radical increase in the conjugate concentration is restricted. Due to this, the majority of specific antibodies that bind in the TZ are not associated with the label. To involve them in the generation of the detected signal, an additional stage was proposed.

Preprints (www.preprints.org) | NOT PEER-REVIEWED | Posted: 28 April 2022 doi:10.20944/preprints202204.0272.v1

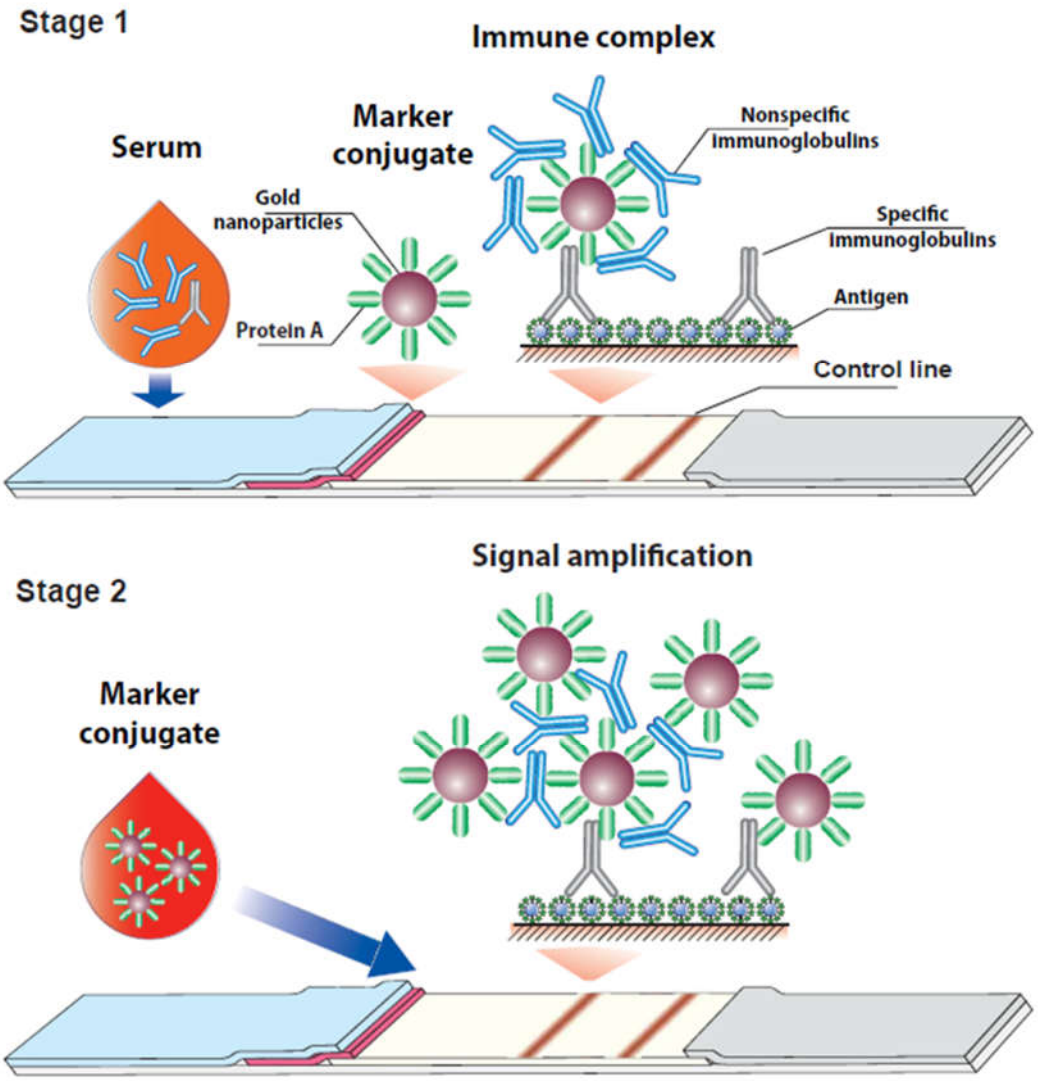

Figure 1. Scheme of the proposed enhanced serodiagnostic LFIA.

At the second stage of the assay, a labeled immunoglobulin-binding protein is added to the working membrane of the test strip. This complex flows along the membranes after the sample thus washing out the unbound immunoglobulins from the working membrane and interacting with the immunoglobulins bound in the TZ. At this stage, the release of the analytical signal occurs in two ways (Fig. 1, stage 2). On the one hand, the labeled immunoglobulin-binding protein interacts with the antibody-antigen complexes in the TZ. On the other hand, the label conjugate bound in the TZ at the first stage provides available sites to bind the added reagent. Because IgG molecules have two symmetric binding sites for immunoglobulin-binding proteins, they could serve for the formation of various polycompound complexes based on the labeled immunoglobulin-binding protein that is initially bound at the TZ and contains a lot of IgG molecules at its surface. In this way, nonspecific immunoglobulins interfere with signal generation at the first stage but provide signal enhancement at the second stage.

In the presented study, the approach proposed for signal amplification and improvement of diagnostics was tested to develop a new LFIA format for the detection of antibodies against the RBD antigen of the SARS-CoV-2.

Preprints (www.preprints.org) | NOT PEER-REVIEWED | Posted: 28 April 2022 doi:10.20944/preprints202204.0272.v1

3.2. Characterization of the conjugate of gold nanoparticles with protein A

Protein A of *Staphylococcus aureus* labeled with gold nanoparticles was used as a reagent for immunoglobulins binding. To characterize the size and homogeneity of nanoparticles, microphotographs were obtained by TEM. Images of nanoparticles are presented in Fig. 2a and the particle size distribution is shown in Fig. 2b. The average size of nanoparticles (171 particles were processed) was 31.51 ± 9.27 nm (minimum value – 16.78 nm, maximum value – 65.16 nm) with an ellipticity of 1.28 ± 0.27. Conjugated nanoparticles were not aggregated in solution; they were stable during storage and drying on a membrane.

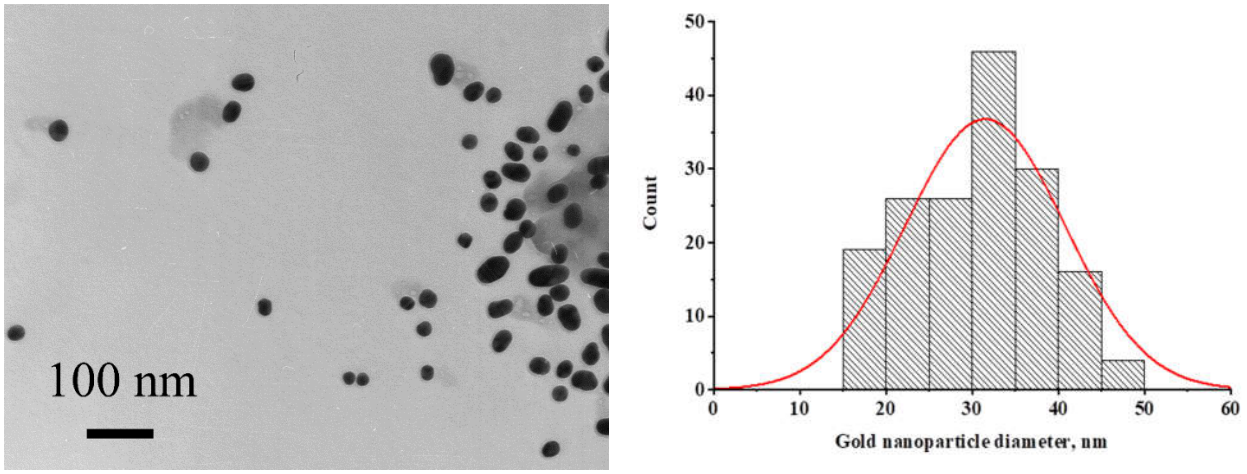

(**a**) (**b**)

Figure 2. (**a**) Micrograph of the conjugate of gold nanoparticles with staphylococcal protein A; (**b**) Histogram of particle size distribution.

3.3. Detection of specific IgG in model solutions

To estimate processes occurring in the proposed two-stage serodiagnostic LFIA and possibilities to detect the lower concentration of specific antibodies in blood samples, the knowledge about the minimal concentration of detectable antibodies is very important. For this purpose, we detected specific antibodies against the SARS-CoV-2 RBD in model solutions. Humanized rat monoclonal antibodies against the RBD were used as analytes. They contained human Fc fragments to most accurately reproduce the behavior of real immunoglobulins in human biosamples. Fig. 3 shows the results of antibody testing by the common LFIA. It was demonstrated that up to 10 ng/mL of specific antibodies can be detected by this method in the absence of non-specific immunoglobulins. The concentration of IgG specific to individual antigens in the blood is usually in a range of 3–50 μg/mL [36-38]. Therefore, the test system has a large margin in sensitivity for antibody detection and the only reason for a possible false-negative test result is signal suppression by non-specific immunoglobulins.

Preprints (www.preprints.org) | NOT PEER-REVIEWED | Posted: 28 April 2022 doi:10.20944/preprints202204.0272.v1

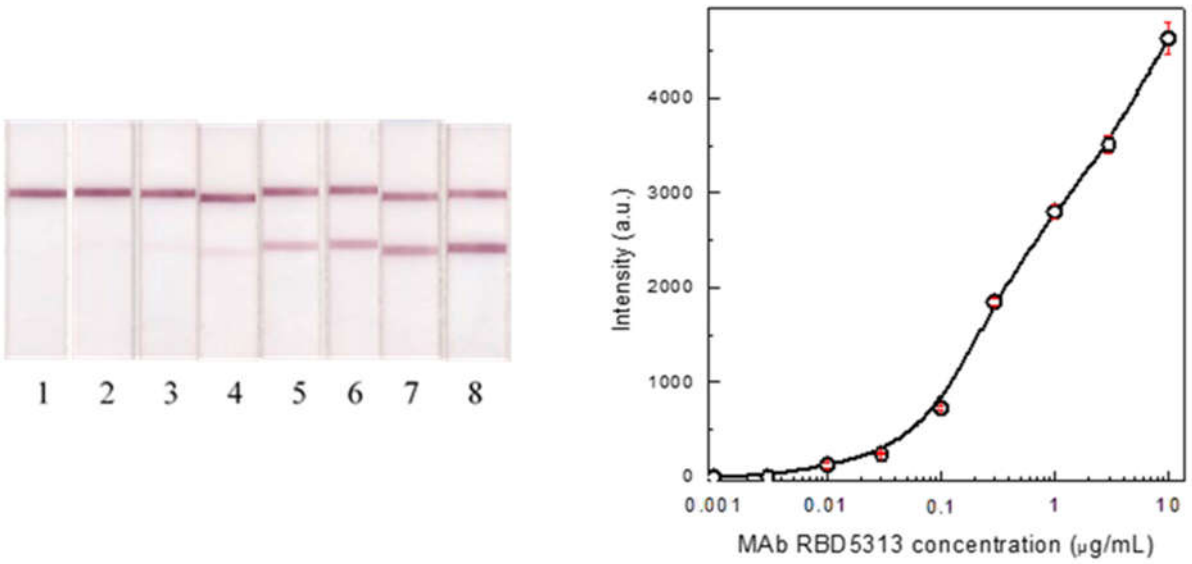

(**a**) (**b**)

Figure 3. Images of test strips (a) after the common LFIA of samples containing 0.003 (1), 0.01 (2), 0.03 (3), 0.1 (4), 0.3 (5), 1 (6), 3 (7), and 10 (8) μg/mL of MAb RBD5313 in PBS and the concentration dependence (b) of the assay (n = 3). Hereafter, top and bottom colored lines on test strips images correspond to the CZ and TZ, respectively.

3.4. The influence of serum components on the LFIA

To evaluate the effect of biosamples' components, primarily, nonspecific immunoglobulins, on the LFIA results, we used pooled serum. The pooled serum was diluted with PBST (1:3-1:100) and Mab against RBD (the same as in the previous section) were added to the model solutions to a final concentration of 10 μg/mL. The mixtures were tested using the common and enhanced LFIAs. The obtained results demonstrated that in the case of the common LFIA, the use of undiluted serum or one diluted less than 6 times led to the decrease of the signal to an undetectable value (Fig. 4a, c (curve I)). Even when the serum was diluted 100 times, the signal was reduced by 8 times relative to that registered after the LFIA in the buffer. After the second stage of the assay, the LFIA signal increased by more than 3 times (Fig. 4b, c (curve II)). The comparison of different serum dilutions demonstrates that a 25-fold dilution of serum is sufficient to achieve the maximum signal.

The obtained data are correlated with the regularities described in the previous study [20], which recommends diluting serum from 10 to 100 times to minimize the effect of non-specific antibodies on the results of common serodiagnostic LFIA. For further studies, sera 25 times diluted with PBST were used as analyzed samples.

Preprints (www.preprints.org) | NOT PEER-REVIEWED | Posted: 28 April 2022 doi:10.20944/preprints202204.0272.v1

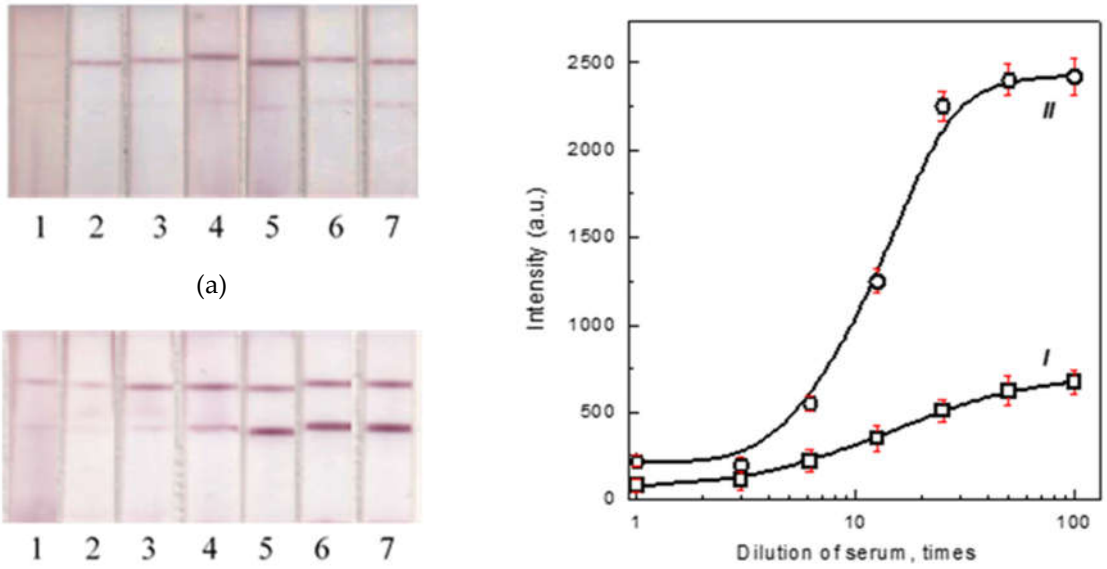

Figure 4. Images of test strips after the common (a) and enhanced (b) LFIA of samples containing 1 (1), 3 (2), 6.2 (3), 12.5 (4), 25 (5), 50 (6), and 100 (7) fold dilutions of pooled negative human serum and 10 μg/mL of monoclonal antibodies against RBD. (c) Concentration dependence of the common (I) and enhanced (II) LFIA (n = 3).

3.5. Comparison of LODs for two formats of the LFIA

Using the chosen dilution of serum samples, the LODs for specific MAb RBD5313 were estimated for the common and enhanced LFIA. The final concentration of the added antibodies varied from 3 ng/mL to 10 μg/mL. When performing the common LFIA, the LOD of specific antibodies in serum was 300 ng/mL, which was 30-fold higher than that when detecting antibodies in a buffer solution with the same test system (Fig. 5a, c (curve I)). After the second stage, the LOD decreased by 30 times (Fig. 5b, c (curve II)). Therefore, in our case, the proposed enhancement strongly eliminates the effect of nonspecific antibodies on the LODs: a 30-fold loss was compensated by a 30-fold improvement. The results also demonstrated that at lower antibody concentrations in the sample, the enhancement at the second stage of LFIA was more manifested as compared with high antibody concentrations (above 1 μg/mL). This fact is especially important for detecting the antipathogen antibodies in weakly positive samples.

Preprints (www.preprints.org) | NOT PEER-REVIEWED | Posted: 28 April 2022 doi:10.20944/preprints202204.0272.v1

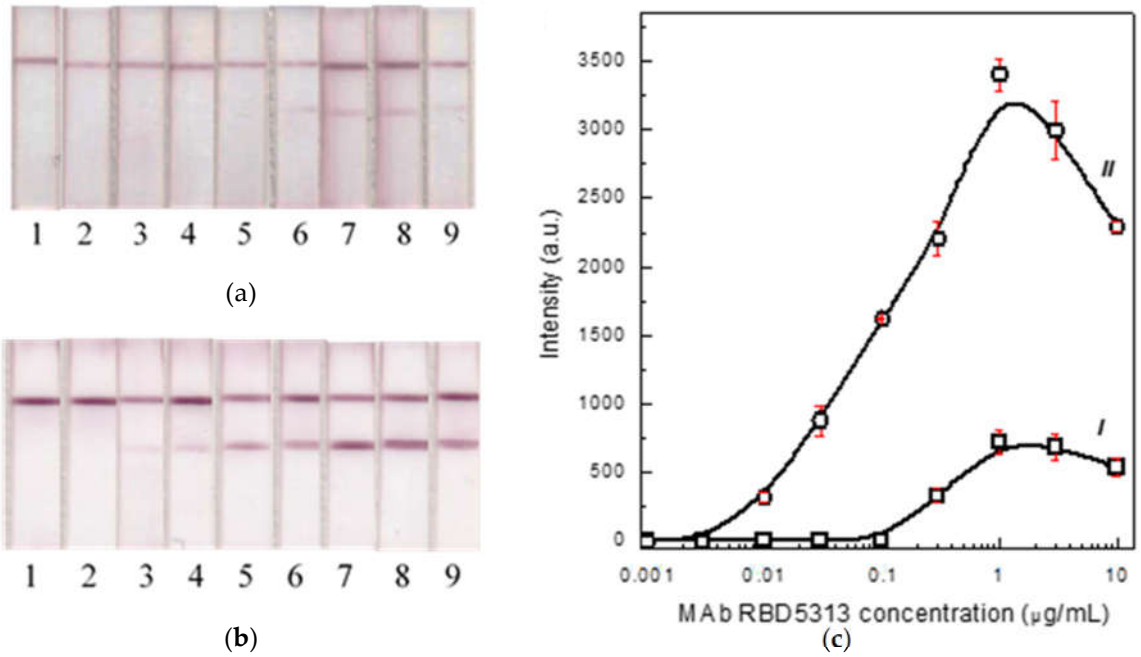

Figure 5. Images of test strips after the common (a) and enhanced (b) LFIA of samples containing 0 (1), 0.003 (2), 0.01 (3), 0.03 (4), 0.1 (5), 0.3 (6), 1 (7), 3 (8), and 10 (9) μg/mL of MAb RBD5313. (c) Concentration dependence of the common (I) and enhanced (II) LFIA (n = 3).

3.6. Determination of the optimal concentration of the label conjugate

As it was already noted, blood immunoglobulins are in large quantitative excess relative to the binding capacity of the label conjugate (considering real ratios of these reactants in the test system). Therefore, the higher the concentration of the conjugate, the higher the sensitivity of the test system. However, an increase in the concentration of colloidal particles increases the likelihood of their aggregation, which reduces the availability of immunoglobulin-binding centers. Thus, the optimal concentration of the conjugate will provide the maximum binding capacity. To find out this concentration, we made a series of test strips that differed in the concentration of the pA-GNP conjugate applied before the first stage of the assay. Fig. 6 shows the testing results of serum samples with a known concentration of specific antibodies by LFIAs differing in concentrations of pA-GNP applied on the test strips (OD_{520} of gold solutions were 2, 5, 10, and 20). The optimal concentration of the conjugate, which provided the maximum analytical signal and the minimum LOD, corresponded to OD_{520} = 10. This conjugate concentration was used in all further experiments.

Preprints (www.preprints.org) | NOT PEER-REVIEWED | Posted: 28 April 2022 doi:10.20944/preprints202204.0272.v1

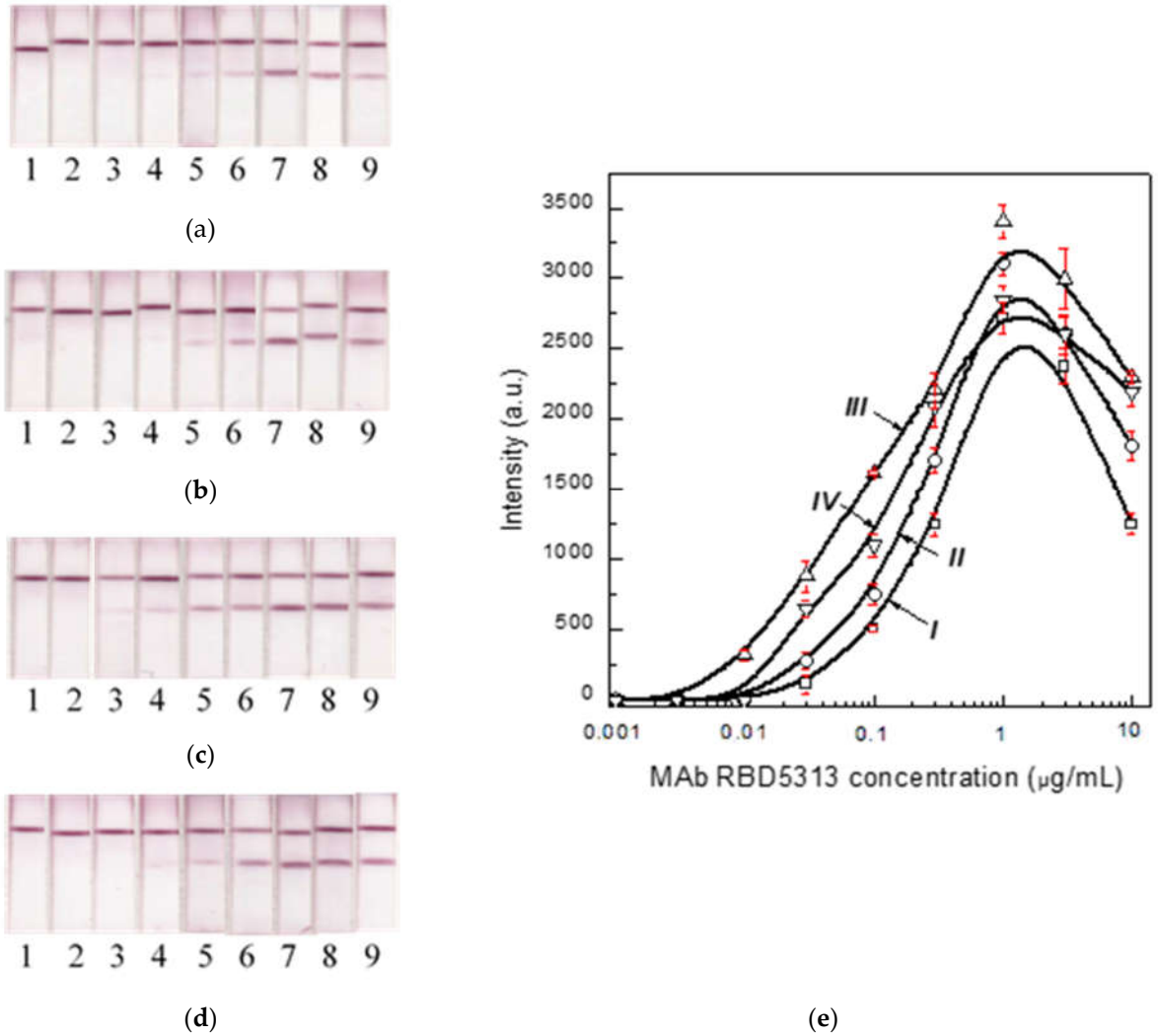

Figure 6. Images of test strips manufactured with the pA–GNP conjugate having OD_{520} = 2 (a), 5 (b), 10 (c), and 20 (d) after LFIA of samples containing 0 (1), 0.003 (2), 0.01 (3), 0.03 (4), 0.1 (5), 0.3 (6), 1 (7), 3 (8), and 10 (9) ng/mL of MAb RBD5313. (e) Concentration dependence for test systems containing the pA–GNP conjugate with OD_{520} = 2 (I), 5 (II), 10 (III), and 20 (IV) (n = 3).

3.7. Testing of the developed LFIAs on blood samples of patients with a confirmed COVID-19 diagnosis

To validate the developed analytical systems, the positive standard of the National Institute for Biological Standards and Control (Hertfordshire, UK) was first used. As shown in Fig. 7, the proposed enhancing approach increased the coloration in the TZ from 6 times to 3 orders of magnitude. The maximum signal was observed in the enhanced LFIA when the serum was diluted from 20 to 40 times.

Preprints (www.preprints.org) | NOT PEER-REVIEWED | Posted: 28 April 2022 doi:10.20944/preprints202204.0272.v1

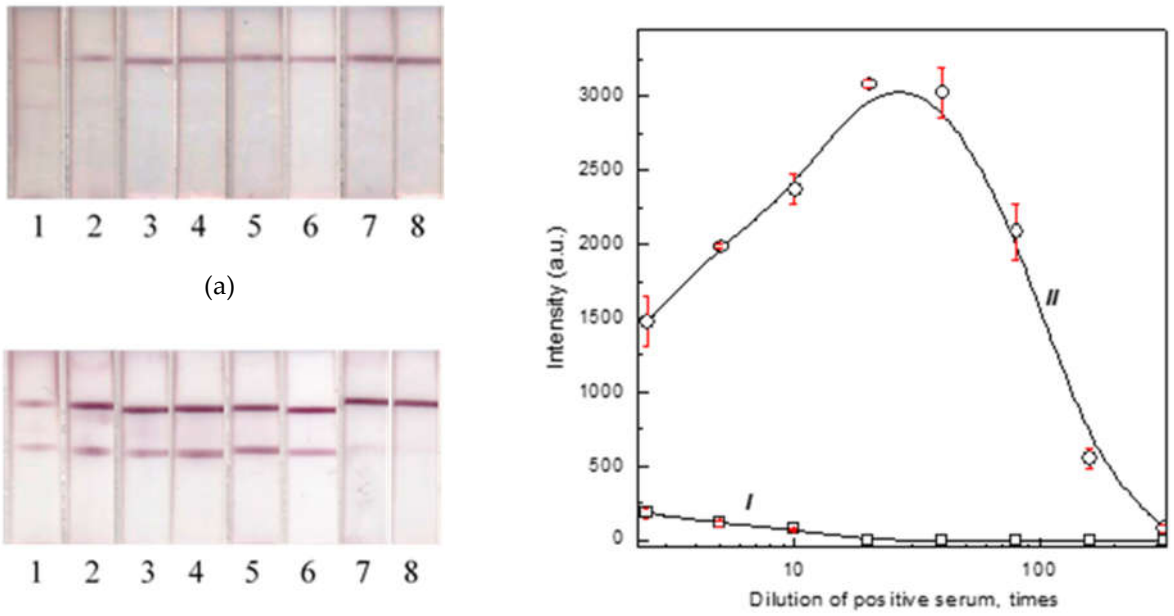

Figure 7. Images of test strips after the common (a) and enhanced (b) LFIAs of samples of pooled human serum containing antibodies to RBD SARS CoV-2 diluted by 2.5 (1), 5 (2), 10 (3), 20 (4), 40 (5), 80 (6), 160 (7), and 320 (8) times. (c) Concentration dependence of the common (I) and enhanced (II) LFIA (n = 3).

After that, the developed LFIAs were compared with the ELISA in terms of the efficiency of detecting specific antibodies in samples from patients. For this, a panel of 24 sera was collected, which included 16 sera from patients with confirmed COVID-19 and 8 negative sera. This panel has been tested by ELISA.

The resulting panel of positive and negative samples was tested by the LFIA in two formats (see Table 1). Samples providing the color intensities of the TZ above 100 arbitrary units (a.u.) (which roughly corresponded to the visual detection threshold) were considered as positive ones. When using the common LFIA, 6 out of 16 positive samples gave negative results (i.e., the diagnostic sensitivity was 62.5%). When using the enhanced LFIA, all 16 ELISA-positive sera gave positive results (with a diagnostic sensitivity of 100%). When testing a panel of negative sera, no positive results were observed (i.e., the diagnostic specificity was 100%).

Preprints (www.preprints.org) | NOT PEER-REVIEWED | Posted: 28 April 2022 doi:10.20944/preprints202204.0272.v1

Table 1. Comparison of ELISA and LFIA data for 24 human serum samples.

Positive sera																
№	1	2	3	4	5	6	7	8	9	10	11	12	13	14	15	16
Common LFIA	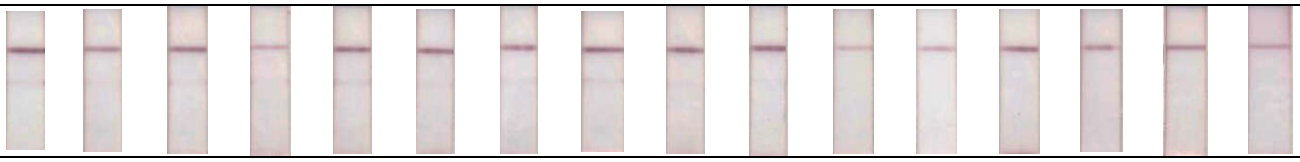															
I (a.u.)	208	135	140	135	155	130	142	180	90	85	0	0	0	0	0	35
	+	+	+	+	+	+	+	+	+	-	-	-	-	-	-	-
Enhanced LFIA	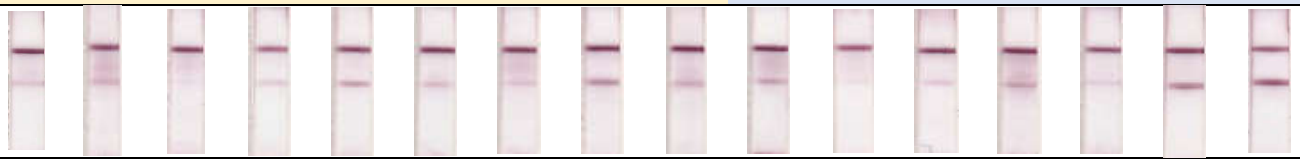															
I (a.u.)	585	635	175	525	1650	1285	880	2520	775	1780	125	956	1430	785	2350	3575
	+	+	+	+	+	+	+	+	+	+	+	+	+	+	+	+
ELISA (A 450)	0.807	1.034	0.299	1.004	1.114	0.957	0.747	1.038	0.848	1.124	0.256	0.730	0.932	0.659	0.899	1.072

Negative sera								
№	1	2	3	4	5	6	7	8
Common LFIA								
I (a.u.)	0	0	0	0	0	0	0	0
	-	-	-	-	-	-	-	-
Enhanced LFIA	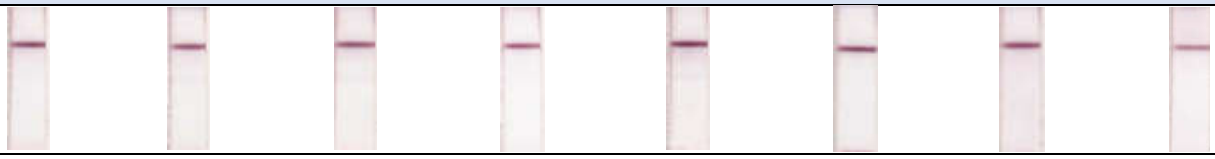							
I (a.u.)	0	65	75	0	55	0	0	0
	-	-	-	-	-	-	-	-
ELISA (A 450)	0.125	0.184	0.198	0.093	0.128	0.120	0.191	0.228

4. Conclusions

The present study demonstrates the critical influence of non-specific immunoglobulins on the diagnostic sensitivity of immunochromatographic serodiagnosis and suggests a way to eliminate this influence. The proposed format of the serodiagnostic LFIA with two stages of signal generation was tested for the COVID-19 serodiagnosis and showed a signal increase up to three orders of magnitude. At the same time, the tested 16 positive

sera showed a decrease in the percentage of false-negative results from 37.5% to 0 compared to the common serodiagnostic LFIA. The total duration of all stages of the proposed assay is 15 min, which fits into the concept of rapid assays. The applicability of the described approach is not limited to a specific pathogen; the proposed solution can be used to increase the sensitivity of serodiagnostic of other diseases.

Author Contributions: Conceptualization, D.V.S., N.A.B., A.V.Z. and B.B.D.; investigation, D.V.S., N.A.B.; methodology, D.V.S., N.A.B., A.V.Z. and B.B.D.; resources, D.V.S., N.A.B.; validation, D.V.S., N.A.B.; visualization, D.V.S., N.A.B. and A.V.Z.; writing (original draft), D.V.S., N.A.B., A.V.Z. and B.B.D.; Writing (review and editing), D.V.S., N.A.B., A.V.Z, Y.X. and B.B.D.

Funding: The reported study was funded by RFBR and NSFC according to the research project № 20-58-55001.

Conflicts of Interest: The authors declare no conflicts of interest.

References

1. Champoux J.J.; Lawrence Drew W.; Neidhardt F.C.; Plorde J.J. Sherris Medical Microbiology, 4th ed.; McGraw-Hill: New York, USA, 2004; 247-249.
2. Lau S.K.P.; He Z.; Tsang C.C.; Chan T.T.Y.; Luk H.K.H.; Chan E.; Li K.S.M.; Fung J.; Chow F.W.N.; Tam A.R.; Chung T.W.H.; Wong S.C.Y.; Que T.L.; Fung K.S.C.; Lung D.C.; Wu A.K.L.; Hung I.F.N.; Teng J.L.L.; Wernery U.; Hui S.W.; Martelli P.; Woo P.C.Y. A sensitive and specific competitive enzyme-linked immunosorbent assay for serodiagnosis of COVID-19 in animals. Microorganisms 2021, 9(5): 1019
3. Elschner M.C.; Laroucau K.; Singha H.; Tripathi B.N.; Saqib M.; Gardner I.; Saini S.; Kumar S.; El-Adawy H.; Melzer F.; Khan I.; Malik P.; Sauter-Louis C.; Neubauer H. Evaluation of the comparative accuracy of the complement fixation test, Western blot and five enzyme-linked immunosorbent assays for serodiagnosis of glanders. PLoS One 2019, 14(4): e0214963.
4. Fortes-Gabriel E.; Guedes M.S.; Shetty A.; Gomes C.K.; Carreira T.; Vieira M.L.; Esteves L.; Mota-Vieira L.; Gomes-Solecki M. Enzyme immunoassays (EIA) for serodiagnosis of human leptospirosis: specific IgG3/IgG1 isotyping may further inform diagnosis of acute disease. PLoS Neglected Tropical Diseases 2022, 16(2): e0010241.
5. Goryacheva I.Y., P. Lenain, S. De Saeger. Nanosized labels for rapid immunotests. TrAC 2013, 46: 30-43.
6. Kwizera R.; Bongomin F.; Olum R.; Worodria W.; Bwanga F.; Meya D.B.; Kirenga B.J.; Gore R.; Denning D.W.; Fowler S.J. Evaluation of an Aspergillus IgG/IgM lateral flow assay for serodiagnosis of fungal asthma in Uganda. PLoS One 2021, 16(5): e0252553.
7. Lu J.; Wu Z.; Liu B.; Wang C.; Wang Q.; Zhang L.; Wang Z.; Chen C.; Fu Y.; Li C.; Li T. A time-resolved fluorescence lateral flow immunoassay for rapid and quantitative serodiagnosis of Brucella infection in humans. J. Pharm. Biomed. Anal. 2021, 200: 114071.
8. Jain M.; Singh A.K.; Kumar A.; Gupta S.; Polavarapu R.; Sohal J.S. Comparative performance of different antigens on the lateral flow assay (LFA) platform for the rapid serodiagnosis of paratuberculosis. J. Microbiol. Methods 2021. 192: 106367.
9. Lempp F.A.; Roggenbach I.; Nkongolo S.; Sakin V.; Schlund F.; Schnitzler P.; Wedemeyer H.; Le Gal F.; Gordien E.; Yurdaydin C.; Urban S. A rapid point-of-care test for the serodiagnosis of hepatitis delta virus infection. Viruses 2021, 13(12): 2371.
10. Anil M.; Navaneetha P.; Reddy, P. V. Janardhan; Chand M. Prudhvi; Kumar A. Vijay; Kishor P. B. Kavi; Rao K. R. S. Sambasiva; Rathnagiri P. Development of point-of-care lateral flow immuno-chromatographic assay for foot and mouth disease diagnosis. Curr. Trends. Biotechnol. Pharm. 2021, 15(1): 15-21.
11. Higgins R.L.; Rawlings S.A.; Case J.; Lee F.Y.; Chan C.W.; Barrick B.; Burger Z.C.; Yeo K.J.; Marrinucci D. Longitudinal SARS-CoV-2 antibody study using the Easy Check COVID-19 IgM/IgG™ lateral flow assay. PLoS One 2021, 16(3): e0247797.
12. Srivastav S.; Dankov A.; Adanalic M.; Grzeschik R.; Tran V.; Pagel-Wieder S.; Gessler F.; Spreitzer I.; Scholz T.; Schnierle B.; Anastasiou O.E.; Dittmer U.; Schlücker S. Rapid and sensitive SERS-based lateral flow test for SARS-CoV2-specific IgM/IgG antibodies. Anal. Chem. 2021, 93(36): 12391-12399.
13. Fu Y.; Pan Y.; Li Z.; Li Y. The utility of specific antibodies against SARS-CoV-2 in laboratory diagnosis. Front. Microbiol. 2021, 11: 603058.
14. Vengesai A.; Midzi H.; Kasambala M.; Mutandadzi H.; Mduluza-Jokonya T.L.; Rusakaniko S.; Mutapi F.; Naicker T.; Mduluza T. A systematic and meta-analysis review on the diagnostic accuracy of antibodies in the serological diagnosis of COVID-19. Syst. Rev. 2021, 10(1): 155.
15. Sotnikov D.V.; Zherdev A.V.; Dzantiev B.B. Lateral flow serodiagnosis in the double-antigen sandwich format: Theoretical consideration and confirmation of advantages. Sensors 2021, 21(1): 39.
16. Yunus M.H.; Arifin N.; Balachandra D.; Anuar N.S.; Noordin R. Lateral flow dipstick test for serodiagnosis of strongyloidiasis. Am. J. Trop. Med. Hyg. 2019, 101(2), 432-435.

17. Prakash C.; Kumar B.; Singh R.P.; Singh P.G.; Shrinet G.; Das A.R.; Ashmi M.; Abhishek Singh K.P.; Singh M.; Gupta V.K. Development and evaluation of a gold nanoparticle based lateral flow assay (LFA) strip test for detection of Brucella spp. J. Microbiol. Methods 2021, 184: 106185.
18. Manasa M.; Revathi P.; Chand M.P.; Maroudam V.; Navaneetha P.; Raj G.D.; Kishor P.B.K.; De B Rathnagiri P. Protein-G-based lateral flow assay for rapid serodiagnosis of brucellosis in domesticated animals. J. Immunoassay Immunochem. 2019, 40(2), 149-158.
19. Di Nardo F.; Chiarello M.; Cavalera S.; Baggiani C.; Anfossi L. Ten years of lateral flow immunoassay technique applications: trends, challenges and future perspectives. Sensors 2021, 21(15): 5185.
20. Sotnikov D.V.; Zherdev A.V.; Dzantiev B.B. Mathematical model of serodiagnostic immunochromatographic assay. Anal. Chem. 2017, 89(8), 4419-4427.
21. Sotnikov D.V.; Berlina A.N.; Zherdev A.V.; Eskendirova S.Z.; Mukanov K.K.; Ramankulov Y.R.; Mukantayev K.N.; Dzantiev B.B. Comparison of three schemes of quantum dots-based immunochromatography for serodiagnosis of brucellosis in cattle. J. Eng. Appl. Sci. 2019, 14, 3711-3718.
22. Karakus C.; Salih B.A. Comparison of the lateral flow immunoassays (LFIA) for the diagnosis of Helicobacter pylori infection. J. Immunol. Methods 2013, 396(1): 8-14.
23. Sotnikov D.V.; Zherdev A.V.; Dzantiev B.B. Theoretical and experimental comparison of different formats of immunochromatographic serodiagnostics. Sensors 2018, 18(1): 36.
24. Martínez-Sernández V.; Muiño L.; Perteguer M.J.; Gárate T.; Mezo M.; González-Warleta M.; Muro A.; Correia da Costa J.M.; Romarís F.; Ubeira F.M. Development and evaluation of a new lateral flow immunoassay for serodiagnosis of human fasciolosis. PLoS Negl. Trop. Dis. 2011, 5(11): e1376.
25. Ben-Selma W.; Harizi H.; Boukadida J. Immunochromatographic IgG/IgM test for rapid diagnosis of active tuberculosis. Clin. Vaccine Immunol. 2011, 18(12), 2090-2094.
26. Wu H.S.; Chiu S.C.; Tseng T.C.; Lin S.F.; Lin J.H.; Hsu Y.H.; Wang M.C.; Lin T.L.; Yang W.Z.; Ferng T.L.; Huang K.H.; Hsu L.C.; Lee L.L.; Yang J.Y.; Chen H.Y.; Su S.P.; Yang S.Y.; Lin S.Y.; Lin T.H.; Su I.S. Serologic and molecular biologic methods for SARS-associated coronavirus infection, Taiwan. Emergi. Infect. Dis. 2004, 10(2), 304-310.
27. Sato N.S.; de Melo C.S.; Zerbini L.C.; Silveira E.P.; Fagundes L.J.; Ueda M. Assessment of the rapid test based on an immunochromatography technique for detecting anti-Treponema pallidum antibodies. Rev. Inst. Med. Trop. Sao Paulo 2003, 45: 319-22.
28. Vrublevskaya V.V.; Afanasyev V.N.; Grinevich A.A.; Skarga Y.Y.; Gladyshev P.P.; Ibragimova S.A.; Krylsky D.V.; Dezhurov S.V.; Morenkov O.S. A sensitive and specific lateral flow assay for rapid detection of antibodies against glycoprotein B of Aujeszky's disease virus. J. Virol. Methods 2017, 249: 175-180.
29. Jia J.; Ao L.; Luo Y.; Liao T.; Huang L.; Zhuo D.; Jiang C.; Wang J.; Hu J. Quantum dots assembly enhanced and dual-antigen sandwich structured lateral flow immunoassay of SARS-CoV-2 antibody with simultaneously high sensitivity and specificity. Biosens. Bioelectron. 2022, 198: 113810.
30. Liu H.; Dai E.; Xiao R.; Zhou Z.; Zhang M.; Bai Z.; Shao Y.; Qi K.; Tu J.; Wang C.; Wang S. Development of a SERS-based lateral flow immunoassay for rapid and ultra-sensitive detection of anti-SARS-CoV-2 IgM/IgG in clinical samples. Sens. Actuators B Chem. 2021, 329: 129196.
31. Panferov V.G.; Byzova N.A.; Biketov S.F.; Zherdev A.V.; Dzantiev B.B. Comparative study of in situ techniques to enlarge gold nanoparticles for highly sensitive lateral flow immunoassay of SARS-CoV-2. Biosensors 2021, 11(7): 229.
32. Sotnikov D.V.; Barshevskaya L.V.; Zherdev A.V.; Eskendirova S.Z.; Mukanov K.K.; Mukantayev K.K.; Ramanculov Y.M.; Dzantiev B.B. Immunochromatographic system for serodiagnostics of cattle brucellosis using gold nanoparticles and signal amplification with quantum dots. Applied Sciences 2020, 10(3): 738.
33. Sinegubova M.V.; Orlova N.A.; Kovnir S.V.; Dayanova L.K.; Vorobiev I.I. High-level expression of the monomeric SARS-CoV-2 S protein RBD 320-537 in stably transfected CHO cells by the EEF1A1-based plasmid vector. PLoS One 2021, 16(2): e0242890.
34. Meulenbroek A. J. Human IgG Subclasses Useful Diagnostic Markers for Immunocompetence. 2008, 2nd ed.; CLB, 2002; 52.
35. Sotnikov D.V.; Byzova N.A.; Zherdev A.V.; Dzantiev B.B. Retention of activity by antibodies immobilized on gold nanoparticles of different sizes: Fluorometric method of determination and comparative evaluation. Nanomaterials 2021, 11(11): 3117.
36. Kemper M.J.; Altrogge H.; Ganschow R.; Müller-Wiefel D.E. Serum levels of immunoglobulins and IgG subclasses in steroid sensitive nephrotic syndrome. Pediatr. Nephrol. 2002, 17(6), 413-417.
37. Tuerlinckx D.; Florkin B.; Ferster A.; De Schutter I.; Chantrain C.; Haerynck F.; Philippet P.; Strengers P.; Laub R. Pneumococcal antibody levels in children with PID receiving immunoglobulin. Pediatrics 2014, 133(1), e154-e162.
38. Turner P.; Turner C.; Green N.; Ashton L.; Lwe E.; Jankhot A.; Day N.P.; White N.J.; Nosten F.; Goldblatt D. Serum antibody responses to pneumococcal colonization in the first 2 years of life: Results from an SE Asian longitudinal cohort study. Clin Microbiol Infect. 2013, 19(12), E551-E558.